https://arabjchem.org

ScientificScholar®
Knowledge is power
Publisher of Scientific Journals

Arabian Journal of Chemistry

Article in Press

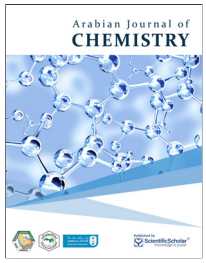

Original Article

Synchronous extraction and separation of corn silk bioactive substance and the prediction of partition efficiency

Jiawei Xu[a,b], Yang Lu[a,b,*]

[a]Key Laboratory of Preparation and Application of Environmental Friendly Materials, Jilin Normal University, Ministry of Education, Siping, 136000, China
[b]Jilin Provincial Key Laboratory for Numerical Simulation, Jilin Normal University, 1301 Haifeng Street, Siping, 136000, China.

ARTICLE INFO

Keywords:
Extraction
Flavonoid
Polysaccharide
Prediction
Separation

ABSTRACT

Flavonoids and polysaccharides are useful components of corn silk. For synchronously extracting and separating the flavonoids and polysaccharides from corn silk, the method of ultrasonic cell disruption extraction was combined with an aqueous two-phase system (ATPS). The separation of flavonoids and solvents, and the recycling of solvents can be achieved by utilizing smart polymers for phase-forming in ATPS. This method presents better extraction efficiency and recycling ability compared to others. The average extraction efficiency for flavonoid and corn silk polysaccharides can reach 16.73 $mg \cdot g^{-1}$ and 75.82 $mg \cdot g^{-1}$. The recycling experiment demonstrates the feasibility of using the smart polymer for recycling. The prediction of partition efficiency of the corn silk bioactive substance was implemented by an artificial neural network (ANN) and response surface methodology (RSM). The ANN model outperformed the RSM one in both prediction accuracy and generalization ability.

1. Introduction

Corn silk is a biological by-product of the corn plant (*Zea mays* L.), which belongs to the family Poaceae (Gramineae). Corn silk is the elongated stigmata of the female maize flower, and it is a silky component growing on the ear of the corn. It looks like a bundle of soft threads about 10-20 cm long. The color of corn silk is initially light green and gradually turns yellow, red, or light brown. Corn silk has been used as a herbal remedy in some countries like China, Turkey, United States, and France [1-3]. Although the value of corn silk is widely recognized in traditional medicine, it is not widely used. Corn silk contains a variety of antioxidants and phytoconstituents, including flavonoids, polysaccharides, anthocyanins, tannins, carotenoids, and others. Corn silk contains plenty of flavonoids, and the content ranges from 0.1% to 3% [4]. Studies have shown that flavonoids are potent candidates for disease prevention [5]. Flavonoids have a variety of pharmacological properties, including antibacterial, antioxidant, and hepatoprotective [6-8]. Polysaccharides have attracted increasing attention owing to their unique pharmacological properties. The bioactivity characteristics of polysaccharides include antioxidative, antidiabetic, anti-glycation, and they improve gastrointestinal movement [9,10]. Tannins participate in several biological activities, having bacteriostatic, free radical-scavenging, and antioxidant properties [11,12]. Anthocyanins show antioxidant and antiradical activities [13]. The anthocyanins have certain pharmacological activities such as anti-cancer, anti-diabetic, and hepatoprotective activities [14]. Carotenoids from corn silk have anti-inflammatory, antifungal, and immune-boosting properties [15]. The extraction of effective components from corn silk is crucial for the complete utilization of its resources. Research indicates that flavonoids and polysaccharides are the two main effective components of corn silk. Therefore, the extraction and separation of flavonoids and polysaccharides is a worthwhile endeavor for both research and production.

Recently, several studies have been published on the extraction of biologically active corn silk. However, these studies reported methods for extracting only a single substance, either polysaccharide or flavonoid. Most of the flavonoids and polysaccharides were obtained by ethanol extraction [16], hot water extraction [17], ion exchange [18], expanded bed adsorption [19], and microwave, ultrasonic, and enzyme-assisted methods [20]. However, the single method was not particularly effective due to higher temperature, longer extraction time, and excess energy consumption. Moreover, these articles all reported methods for extracting only a single substance, either polysaccharide or flavonoid.

We attempted to extract flavonoids and polysaccharides simultaneously and then realize their separation. This was achieved by combining ultrasonic cell disruption extraction, aqueous two-phase separation, and high performance liquid chromatography (HPLC) determination. Although this method performed quite well, practical application is still challenging. One is organic solvent recycling, and the other is the subsequent separation of flavonoids from them. Smart polymers [21], also called stimulus-responsive polymers or environmentally sensitive polymers, have been used in aqueous two-phase systems (ATPS) in recent years. These materials possess unique characteristics, exhibiting reversible structural changes at the molecular level, particularly within functional polymer segments [22]. These changes occur when there is a slight change in external environmental factors, such as pH value [23], temperature [24], or magnetic fields [25]. These molecular changes manifest macroscopically as alterations in the solubility in aqueous solutions, changes in the volume of polymer

*Corresponding author:
E-mail address: luyang33@126.com (Y. Lu)

Received: 23 December, 2024 **Accepted:** 10 March, 2025 **Epub Ahead of Print:** 09 May 2025 **Published:** ***
DOI: 10.25259/AJC_308_2024

hydrogels, and changes in moisture content. The object material can be separated from the smart polymer using stimulus-responsive sensitivity. The smart polymer can then be recycled. Thermosensitive polymers are by far the most widely applied smart polymers for two reasons. First, the temperature change is easy to implement. Second, the chemical composition of the system does not change with a change in temperature. The structures of polysaccharides obtained by different extraction methods and conditions vary greatly [26,27]. As an important thermosensitive polymer, poly(ethylene glycol-ran-propylene glycol) monobutyl ether (UCON) has the advantages of manipulative thermosensitivity, proven manufacturing technology, and low cost. It can be introduced into ATPS as a phase-forming polymer. Thus, the problem of separation and recovery of the extraction solvent was solved by using the smart polymer UCON-based ATPS in this study.

Starting with bionics, the artificial neural network (ANN) mimics the manner in which the human brain functions [28]. Human brain neurons were abstracted as cells. Because ANNs have many advantages, such as an adaptive structure, adjustable parameters, and easy training, they have become a mainstream machine learning technology. ANNs have exhibited notable intelligence features when applied to solve complex problems in fields such as pattern recognition, automatic control, biology, medicine, and economics. In recent years, ANNs have been introduced into the field of chemistry, opening up new methods for predicting chemical reaction parameters, compound characteristics, and material performance [29]. Kite *et al.* [30] predicted the productive rate of styrene and other byproducts in the oxidative dehydrogenation of ethylbenzene using an ANN model.

As a potential separation and extraction technique, ATPS [31] has excellent performance in the field of material separation, including proteins [32,33], cytochromes [34], amino acids [35], genetic material [36], polypeptides [37,38], enzymes [39,40], antibiotics [41], chemical materials [42], and metal ions [43,44]. The prediction of separation efficiency has always been the focus of ATPS extraction research. Currently, the prediction model was built using response surface methodology (RSM). Studies on intelligent prediction using deep learning technologies have not been reported. In this study, a prediction model for separation efficiency was built using RSM and ANN. Their prediction performances and generalization abilities were studied and compared with those of previously reported methods [45-50].

In this study, the ultrasonic cell disruption extraction and smart polymer UCON-based ATPS separation were investigated for a synchronous extraction and separation of corn silk bioactive substances. This technology solved the problem of separation of flavonoids from the extraction solvent. At the same time, the recovery and utilization of the extraction solvent were realized. The optimal extraction and separation conditions were discussed through multi-factor experiments. The separation prediction model was established by two methods, namely RSM and ANN. The antioxidant activities of the flavonoids and corn silk polysaccharides were studied by determining the DPPH free radical scavenging activities, superoxide radical scavenging abilities, and hydroxyl radicals' inhibitory activities. This method of synchronous extraction and separation of Corn silk bioactive substance was compared with extraction methods described in previous literature to verify the validity of the method. The prediction performances and generalization abilities of the prediction model were compared with other models.

2. Materials and Methods

2.1. Materials

UCON (average M_n ~3,900) was obtained from Sigma-Aldrich Co., Ltd. (Shanghai, China). Sulfuric acid (GR, 95.0 ~ 98.0%), acetonitrile (HPLC grade), potassium carbonate (GR, 99.0%), sodium hydroxide (GR, 99.0%), potassium hydrogen phosphate (AR, 99.0%), aluminum chloride (AR, 99.0%), ammonium hydrogen phosphate (AR, 99.0%), ammonium dihydrogen phosphate (GR, 99.5%), sodium nitrite (AR, 99.0%), potassium oxalate (GR, 99.5%), and potassium tartrate (AR, 99.0%) were purchased from Sinopharm Chemical Reagent Co., Ltd. (Shanghai, China). Rutin standard samples were obtained from the Chinese National Institute for the Control of Pharmaceutical and Biological Products (Beijing, China). Analytical-grade phenol and glucose anhydrase were purchased from Shanghai Macklin Biochemical Co., Ltd. (Shanghai, China). 1,1-diphenyl-2-picrylhydrazyl (DPPH, 97%), Tris-HCL (pH 8.0), $FeSO_4$ (0.1 mol/L), H_2O_2 (30 wt.% in H_2O), salicylic acid (AR, 99.5%), and pyrogallol (AR) were obtained from Aladdin Reagent Co., Ltd. (Shanghai, China).

2.2. Apparatus

The ultrasonic cell disruption instrument used for sample pre-treatment was provided by Shanghai Hanuo Instrument Co., Ltd. (HN99-IID, China). An ultraviolet-visible (UV-Vis) spectrophotometer was purchased from SHIMADZU Co., Ltd. (UV2500, Japan). The thermostatic water bath used to control the ATPS temperature was purchased from Zhuocheng Instrument Technology Co., Ltd. (SYP, China). The vacuum freezing dryer used to dry the corn silk was purchased from Shanghai Tianfeng Industrial Co., Ltd. (TF-FD-27, China). The centrifuge was provided by Xiangtan Xiangyi Instrument Co., Ltd. (Cence-H1650, Xiangtan, China). The analytical balance used for weighing was purchased from Mettler Toledo Technology (China) Co., Ltd. (Balance XPR106DUHQ/AC, China), and its uncertainty was $\pm 1.0 \times 10^{-7}$ kg.

2.3. Preparation of corn silk samples

From late July to early August, mature corn silks were handpicked from a pollution-free farm in Siping. A yellow corn variety was used. The corn silks were rinsed and dried under shade for 72 hrs, and the temperature was controlled at 20 ± 2°C. The corn silks were placed in a grinder to obtain the sample powder. In a beaker, 50 mL of a 10% UCON solution and 50 g of sample powder were added and completely mixed. The corn silk UCON solution was subjected to wall-breaking treatment using an ultrasonic cell disruption instrument. The corn silk UCON solution was placed into separate plastic centrifuge tubes after 30 mins of cell disruption. The centrifugal time and rotation speed were 10 mins and 1200 rpm, respectively. Subsequently 30 mL of a 10% UCON solution was added to the residue after the supernatant fluid was collected. The residue was completely mixed, and wall-breaking treatments were performed for 30 mins. The residue mixture was centrifuged at a rotation speed of 1200 rpm for 10 mins. The supernatant fluid was collected. The two supernatants were mixed together and filtered through a 0.45 μm membrane. The filtrate was a corn silk extract solution, denoted as the UCON-based corn silk extract. This extract solution was moved into brown bottles, and was placed in the refrigerator at 4°C.

2.4. Procedure

The UCON solution (0.3 $g \cdot mL^{-1}$), UCON-based corn silk extract, water, and potassium tartrate (0.25 $g \cdot mL^{-1}$) were added into a colorimetric tube with a certain ratio. The total volume was 10 mL. The colorimetric tubes were in a three-min oscillation and then placed in a thermostatic water bath for 15 mins. At this point, there were two phases in the colorimetric tubes. The volumes of the two phases were recorded, and then they were separated. The concentrations of flavonoids and polysaccharides in the two phases and UCON-based corn silk extract were determined.

The UCON-rich phase was then diluted by adding distilled water. The thermostat water bath which was maintained at 65°C temperature was used to control the formation of the two phases. The top phase was isolated to determine flavonoid concentration when the solution formed two new phases. The extraction efficiency and purity of flavonoids were determined [51]. The recovery efficiency of UCON was also determined.

The salt-rich phase was then transferred to a dialysis tube (8000-14,000 Da). Small molecular impurities, including salts, were removed by dialysing in distilled water. After 24 hrs, the dialyzed solution was concentrated using rotary evaporation. According to the ratio of five-time volume, 90% ethanol was added to the concentrated solution. The solution was well blended and placed for 12 hrs at 4°C to precipitate polysaccharides. Sediments were collected by centrifugation. The collected sediment was dissolved in water. The polysaccharides were resedimented in 80% ethanol, and the sediment was obtained by

centrifugation. Anhydrous ethanol was used to wash the sediment, which was then freeze-dried to obtain corn silk polysaccharide. The purity of the corn silk polysaccharide was determined [16].

In our previous study [52], the phenol-sulfuric acid method was used to determine polysaccharide concentration where glucose anhydrase was used as the standard. This method was used for the determination of corn silk polysaccharides. Flavonoid concentration was measured using the reported method [53]. Rutin was taken as the standard. In the purity and antioxidant experiments, the flavonoid concentration was measured by high performance liquid chromatography with ultraviolet detection (HPLC-UV). The chromatographic separation was carried out on an analytical reversed-phase column (4.6 × 250 mm, 5 μm, Agilent TC-C18 column). 10 μL of sample solution was injected. The column temperature was at 25°C. The mobile phase comprised methanol (A) and 1.0 % acetic acid solution (B). The ratio of A and B was as following: 3:7 (0-8 min), 3:7-5:5 (8-13 min), 5:5 (13-20 min), 5:5-6:5 (20-25 min), 6:5-3:4 (25-35 min), 3:4-1:0 (35-45 min), 1:0- 3:7 (45-50 min), 3:7 (50-60.0 min). The flow rate was 1.0 mL·min^{-1}. UV detection wavelength was 280-350 nm [54]. The entire experimental procedure was shown in Figure 1.

2.5. Determination of parameters

The partition efficiency (PE_n) was used to measure the separation performance of ATPE for the flavonoids (n=1) and corn silk polysaccharides (n=2), and was defined by the following Eq. (1):

$$PE_n\% = \frac{C_n \times V_n}{C_s \times V_s} \times 100 \quad (1)$$

where C_n and V_n are the flavonoid concentration and volume of the upper phase respectively, when n = 1; C_n and V_n are the corn silk polysaccharide concentration and volume of the bottom phase, respectively, when n = 2. C_s and V_s are the concentrations of flavonoids or corn silk polysaccharides in the initial system and the volume of the initial system, respectively; n=1 represents flavonoids, and n=2 represents corn silk polysaccharides.

The extraction efficiency (EE_n) represents the ratio of the extracted materials to corn silk and is defined by the following Eq. (2):

$$EE_n = \frac{m_n}{m_t}, \quad (2)$$

where m represents the mass of materials, n=1 represents flavonoids, n=2 represents corn silk polysaccharides, and t represents corn silk.

The purity of the flavonoids and corn silk polysaccharides was defined using the following Eq. (3):

$$\text{Purity}_n = \frac{C_n \times V_n}{m_n}, \quad (3)$$

where C and V represent the concentration and volume of materials in the purity test, respectively, m represents the total mass, n=1 represents flavonoids, and n=2 represents corn silk polysaccharide.

The proposed ANN and RSM models were evaluated using the mean relative percent deviation (MRPD) expressed as follows in Eq. (4):

$$\text{MRPD} = \frac{100}{n}\sum_{i=1}^{n}\left|\frac{y_{c,i} - y_{e,i}}{y_{e,i}}\right|, \quad (4)$$

where 'n' and 'i' were the total amount of data and the data number in the dataset, respectively, y was the response, 'c' was the computational data, and 'e' was the experimental data.

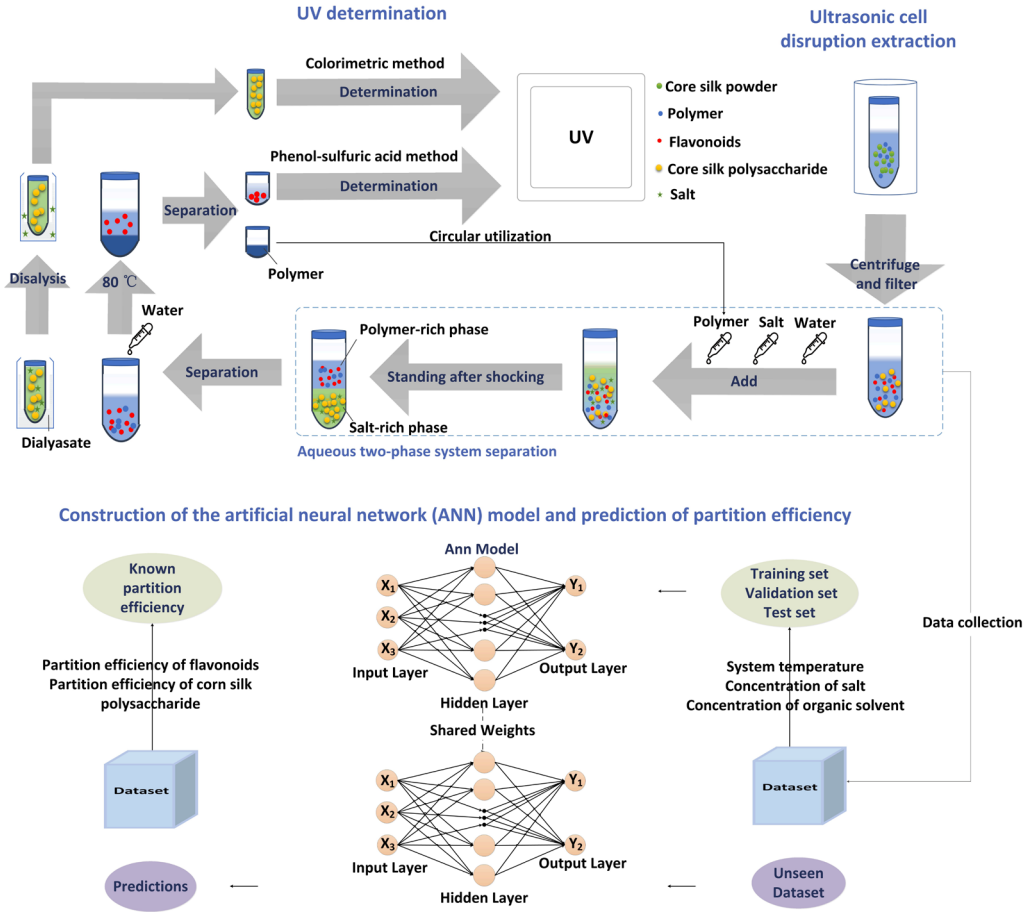

Figure 1. Technology roadmap.

2.6. Antioxidant activity

The antioxidant activities of the flavonoids and corn silk polysaccharides were studied. The 2,2-Diphenyl-1-picrylhydrazyl (DPPH) free radical scavenging activities of the flavonoids and corn silk polysaccharides were evaluated using the reported method [17]. 2.5 mL DPPH solution was added to 1.0 mL of flavonoids or corn silk polysaccharide solution (0.025-0.175 mg·mL^{-1}). They were then completely mixed. Absorbance (A_i) was recorded at 517 nm after 30 mins. The absorbance of the reaction without the sample was denoted as A_c, and the absorbance of anhydrous ethanol was denoted as A_b. The clearance rate was calculated as follows in Eq. (5):

$$\text{Clearance rate (\%)} = \left[1 - \frac{(A_i - A_b)}{A_c}\right] \times 100. \quad (5)$$

The superoxide radical scavenging abilities of the flavonoids and corn silk polysaccharides were determined using the reported method [55]. 1.0 mL of flavonoids or corn silk polysaccharide solution (0.025-0.175 mg·mL^{-1}) was added to seven tubes, which included 3.0 mL ultrapure water and 4.2 mL Tris-HCL (50 mmol·L^{-1}, pH 8.0). The mixture was shaken and then placed at 25°C for 30 mins. The mixture was shaken after adding 0.3 mL pyrogallol (3 mmol·L^{-1}). The absorbance was measured at a wavelength of 325 nm every 30 seconds, resulting in a total of 10 measurements. The rate of absorbance change (F_x) with time was calculated. The change rate (F_0) was obtained without the sample. The clearance rate was calculated as follows in Eq. (6):

$$\text{Clearance rate (\%)} = \left[1 - \frac{F_x}{F_0}\right] \times 100. \quad (6)$$

The hydroxyl radicals inhibitory activities of the flavonoids and corn silk polysaccharides were quantified using the reported method [20] with minor modifications. Salicylic acid ethanol (2.0 mL) (9 mmol·L^{-1}) and $FeSO_4$ (2.0 mL) (9 mmol·L^{-1}) were added to 1.0 mL flavonoids or corn silk polysaccharide solution (0.025-0.175 mg·mL^{-1}). Then, 2.0 mL H_2O_2 (8.5 mmol·L^{-1}) was added to the mixture. The tubes were placed at 35°C for 20 mins. The absorbance (A_x) was determined at 510 nm, and the absorbance of the reaction without the sample was denoted as A_y. The absorbance of the distilled water was denoted as A_0 (Eq. 7).

$$\text{Clearance rate (\%)} = \left[1 - \frac{(A_x - A_y)}{A_0}\right] \times 100 \quad (7)$$

2.7. Statistical analysis

The range of conditions for the multifactor experiment was obtained by analyzing the results of the single-factor test. The factorial design of the multifactor experiment was created using Design-Expert 10.0, according to the RSM. The Central Composite Design (CCD) method was used to perform the experimental design, and there were three factors with five levels, as described next. The first independent factor was the UCON concentration, represented by X_1; the second factor was the $K_2C_4H_4O_6$ concentration, represented by X_2; and the third factor was the system temperature, represented by X_3. Regression analysis was performed using Design-Expert 10.0, and the analysis model used was a quadratic equation (Eq. 8) as follows:

$$Y = \beta_0 + \sum_i \beta_i X_i + \sum_i \beta_{ii} X_i^2 + \sum_{ij} \beta_{ij} X_i X_j, \quad (8)$$

where X_i and X_j are the factors, and the values of 'i' and 'j' are 1 (concentration of UCON), 2 (concentration of $K_2C_4H_4O_6$), and 3 (system temperature), respectively; Y is the response; β_0 is the intercept; β_i, β_{ii}, and β_{ij} are the regression coefficient for linear, quadratic, and interaction, respectively; The validity of the model was evaluated based on statistical significance, which was achieved using an *F-test*.

2.8. ANN modeling

The extraction and separation processes were simulated using the developed backpropagation ANN model, as shown in Figure 1. The input layer had three artificial neurons, which represented three factors in the RSM. The output layer had two artificial neurons; the extraction efficiencies of flavonoids (Y_1) and the extraction efficiencies of corn silk polysaccharides (Y_2). The number of artificial neurons was determined by testing in the hidden layer (Figure S1).

The input and output variables were normalized in this ANN model. The three commonly used methods for unification are as follows in Eq. (9) to (11):

$$X' = \frac{X - X_{min}}{X_{max} - X_{min}} \quad (9)$$

$$X' = 0.1 + 0.8 \times \frac{X - X_{min}}{X_{max} - X_{min}} \quad (10)$$

$$X' = 0.1 + 0.8 \times \frac{\log(X - X_{min})}{\log(X_{max} - X_{min})}, \quad (11)$$

where X represents the original data, X′ represents unified values, X_{max} is the original maximum value, and X_{min} is the original minimum value. The training parameters of this ANN model have been listed in Table S1. The best sets of weights were obtained using a cross-validation technique to prevent overtraining.

3. Results and Discussion

3.1. Ultrasonic UCON-extraction efficiency

3.1.1. The effect of UCON concentration

The wall of corn silk was broken by ultrasonic waves, and the effective components in the corn silk were extracted in a UCON solution. The effect of the UCON concentration on the extraction efficiencies of the two objects has been discussed in Table S2. On the one hand, the data showed that an increase in the UCON concentration improved the extraction efficiencies of flavonoids. On the other hand, the influence of UCON concentration on the extraction efficiencies of corn silk polysaccharides was very weak. It was found that the extraction efficiency of flavonoids increased as the concentration changed from 0 to 30%. When the concentration changed from 0 to 10%, the extraction efficiency changed from 17.02 mg·g^{-1} to 19.05 mg·g^{-1}. However, the concentration increased from 10% to 30%, and the extraction efficiency increased by only 0.14 mg·g^{-1}. When the concentration exceeds 30%, the solution is too viscous and not conducive to extraction operations. The reasons for choosing 10% UCON solution as the extraction reagent were the following: (i) the gap in the extraction efficiencies of the two objects between the 10% and 30% UCON solutions was small and (ii) an appropriate concentration of UCON is not only beneficial for improving extraction efficiency but also conducive to the subsequent establishment of an ATPS. Therefore, the concentration of UCON was set to 10%.

3.1.2. The effect of cell disruption time

The cell disruption extraction time had an important effect on the extraction efficiencies of the two objects. In this study, we employed a dual-step cell disruption extraction approach. The research design and experimental results have been presented in Table S3. Overall, the longer the total cell disruption extraction time, the better the extraction efficiencies of the two objects. Specifically, the extraction efficiencies of the two objects were satisfactory when both cell disruption extractions took longer than 30 mins. Therefore, the final condition was set as follows: the time was 30 mins in both cell disruption extractions.

3.2. Choice of salt in UCON-based ATPS

UCON-based corn silk extract was obtained from corn silk *via* cell disruption extraction. A UCON-based ATPS was then used to separate flavonoids and corn silk polysaccharides. Based on the phase formation mechanism of ATPS, we selected 13 salts to construct the ATPS. Six UCON-based ATPS containing different salts were used to separate

flavonoids and corn silk polysaccharides because the mechanisms of extraction and separation in the ATPS were mainly salting-out and rule of similarity. The reason for the choice of six types of UCON-based ATPS was that these six salts have excellent performances. The partition efficiencies of the UCON-based APTSs have been shown in Figure S2. K_2CO_3-UCON-ATPS, K_2HPO_4-UCON-ATPS, and $K_2C_4H_4O_6$-UCON-ATPS showed superior abilities in the separation of flavonoids and corn silk polysaccharides. We used $K_2C_4H_4O_6$-UCON-ATPS as the separation system because $K_2C_4H_4O_6$ was degradable in this study. Furthermore, the degradation components have no adverse effects on the environment.

3.3. Material distribution in UCON-$K_2C_4H_4O_6$ ATPS

3.3.1. The effect of UCON concentration

The concentrations of the two phase-forming materials significantly influenced the phase behavior and object distribution in the two phases. The effects of UCON on the partition efficiency of the objects were studied. The variation trend of the partition efficiency of the two objects with the UCON concentration has been shown in Figure S3. It was found that the partition efficiencies of two objects increased with the UCON concentration changing from 0.045 g·mL^{-1} to 0.165 g·mL^{-1}. This was because more flavonoids were brought to the upper phase by UCON with an increase in UCON concentration. Meanwhile, the UCON concentration increased, and the water content decreased in the upper phase. Corn silk polysaccharide was a water-soluble polysaccharide, and it was easier to enter the lower phase that was rich in water. However, the ATPS will appear as a salting-out phenomenon when the UCON concentration is above 0.180 g·mL^{-1}. Therefore, the UCON concentration was set as between 0.070 g·mL^{-1} and 0.175 g·mL^{-1} in multi-factor experimental.

3.3.2. The effect of $K_2C_4H_4O_6$ concentration

As another material for forming two phases, the $K_2C_4H_4O_6$ concentration also affects the partition efficiency of the object. The influence of $K_2C_4H_4O_6$ concentration on the partition efficiencies of the objects has been shown in Figure S4. The partition efficiency of flavonoids improved when $K_2C_4H_4O_6$ concentration increased from 0.035 g·mL^{-1} to 0.110 g·mL^{-1}. The salting-out ability was enhanced as the $K_2C_4H_4O_6$ concentration increased. The enhancement of the salting-out ability caused more UCON to be pushed into the upper phase. Subsequently, more flavonoids were taken up to the upper phase by UCON. Therefore, the partition efficiency of flavonoids increased with $K_2C_4H_4O_6$ concentration rising. The partition efficiency of the corn silk polysaccharide first increased and then decreased with increasing $K_2C_4H_4O_6$ concentration. This is because the $K_2C_4H_4O_6$ concentration in the lower phase increased as the $K_2C_4H_4O_6$ concentration increased in the entire system. The ability of corn silk polysaccharide to combine with water was lower than that of the electrolyte ($K_2C_4H_4O_6$). As the $K_2C_4H_4O_6$ concentration increased in the lower phase, more water was combined with $K_2C_4H_4O_6$. Therefore, the corn silk polysaccharide was transferred to the upper phase containing free water from the lower phase, which lacks free water.

3.3.3. The effect of temperature

As an important factor affecting the formation of two aqueous phases for UCON-based ATPSs, the temperature also affects the material distribution in the two phases. The partition efficiencies of the two objects at different temperatures have been shown in Figure S5. It was found that the partition efficiencies of two objects all increased while the temperature changed from 15°C to 35°C. According to previous studies, higher temperatures are beneficial for the UCON-based ATPSs forming [56]. Thus, when the temperature increased, more flavonoids were taken into the top phase by UCON, and the partition efficiencies of the flavonoids increased. Conversely, more UCON moved to the top phase with increasing temperature; therefore, free water increased in the bottom phase. Therefore, it is easier for the water-soluble corn silk polysaccharides to remain in the bottom phase.

3.4. The multi-factor experiment and RSM modeling

3.4.1. The regression model

The design of a multifactor experiment with three factors at five levels was performed using RSM. The multifactor experimental data have been provided in Table S4. Multiple regression analysis was used to analyze the response function (Eq. 8). The significance of each response function coefficient was evaluated. For the two objects, the final partition efficiency prediction models (Eqs. 12 and 13) can be obtained as follows:

$$\begin{aligned} Y_1 = {} & 0.78 + 0.021 \times X_1 + 0.081 \times X_2 + 0.048 \times X_3 \\ & + 0.001 \times X_1 \times X_2 + 0.002 \times X_1 \times X_3 - 0.007 \times X_2 \times X_3 \\ & + 0.002 \times X_1^2 - 0.035 \times X_2^2 + 0.013 \times X_3^2 \end{aligned} \quad (12)$$

$$\begin{aligned} Y_2 = {} & 0.87 + 0.009 \times X_1 + 0.009 \times X_2 + 0.027 \times X_3 \\ & - 0.003 \times X_1 \times X_2 + 0.003 \times X_1 \times X_3 - 0.003 \times X_2 \times X_3 \\ & - 0.009 \times X_1^2 - 0.043 \times X_2^2 - 0.014 \times X_3^2 \end{aligned} \quad (13)$$

In the above prediction equations, Y_1 and Y_2 represent the partition efficiency of the two objects; X_1, X_2, and X_3 are the same as those in Eq. (4). For these three equations, the *R*-square values were 0.7520 and 0.8052. We attempted to obtain better results. Therefore, the quadratic equation was replaced with the quartic equation used in our previous study, and the *R*-square values can reach 0.9568 and 0.9656, respectively. However, the quartic equation as a prediction equation yields very poor prediction results. The analysis shows that the quartic equation over-fit the experimental data. Therefore, the quadratic equation was used as the regression model.

3.4.2. The analysis of model

The normal plots of the residuals of the two models have been shown in Figure S6. All points are distributed in limited areas near the line in subgraph (a). Almost all the points are distributed in the vicinity of one straight line in subgraph (b). This illustrates the small deviation between the experimental data and the prediction results for the partition efficiency model of the two objects. In the analysis of the variance process, the evaluation of the statistical analysis of the two partition efficiency models was performed using Fisher's *F-test*. The details of the evaluation have been presented in Table S5. It was found that the values "*p-value* Prob>F" are less than 0.05 in these two models, which illustrated that they are significant. In the partition efficiency model of two objects, the "*p-value* Prob>F" of lack of fit are all greater than 0.05, and these showed that lack of fit is not significant. Based on the above analysis, the regression equations have a satisfactory fitting effect and credibility.

3.4.3. The combined effect of three factors

Response surface plots were used to show the combined effect of the factors on the partition efficiency, as shown in Figure 2. From this figure, the optimum ranges for the two variables were obtained. The optimal values of the two responses can be determined based on Figure 2 and Table S4. The observations were as follows: the partition efficiencies of the flavonoid were 92.62% when the UCON concentration, $K_2C_4H_4O_6$ concentration, and temperature were 0.15 mg·mL^{-1}, 0.0875 mg·mL^{-1}, and 35°C, respectively. The partition efficiency of corn silk polysaccharide was 88.59% when the UCON concentration, $K_2C_4H_4O_6$ concentration, and temperature were 0.12 mg·mL^{-1}, 0.0625 mg·mL^{-1}, and 42°C, respectively. A higher concentration of $K_2C_4H_4O_6$ was beneficial for the partition efficiencies of the flavonoid, but the partition efficiency of corn silk polysaccharide decreased when the concentration of $K_2C_4H_4O_6$ was over 0.08 mg·mL^{-1}. Considering the balance between two objects and mild conditions, the optimal experimental conditions were: UCON concentration was 0.15 mg·mL^{-1}, $K_2C_4H_4O_6$ concentration was 0.07 mg·mL^{-1}, and temperature was 35°C. Under these conditions, the partition efficiencies of the two objects reached 91.18% and 88.67%, respectively.

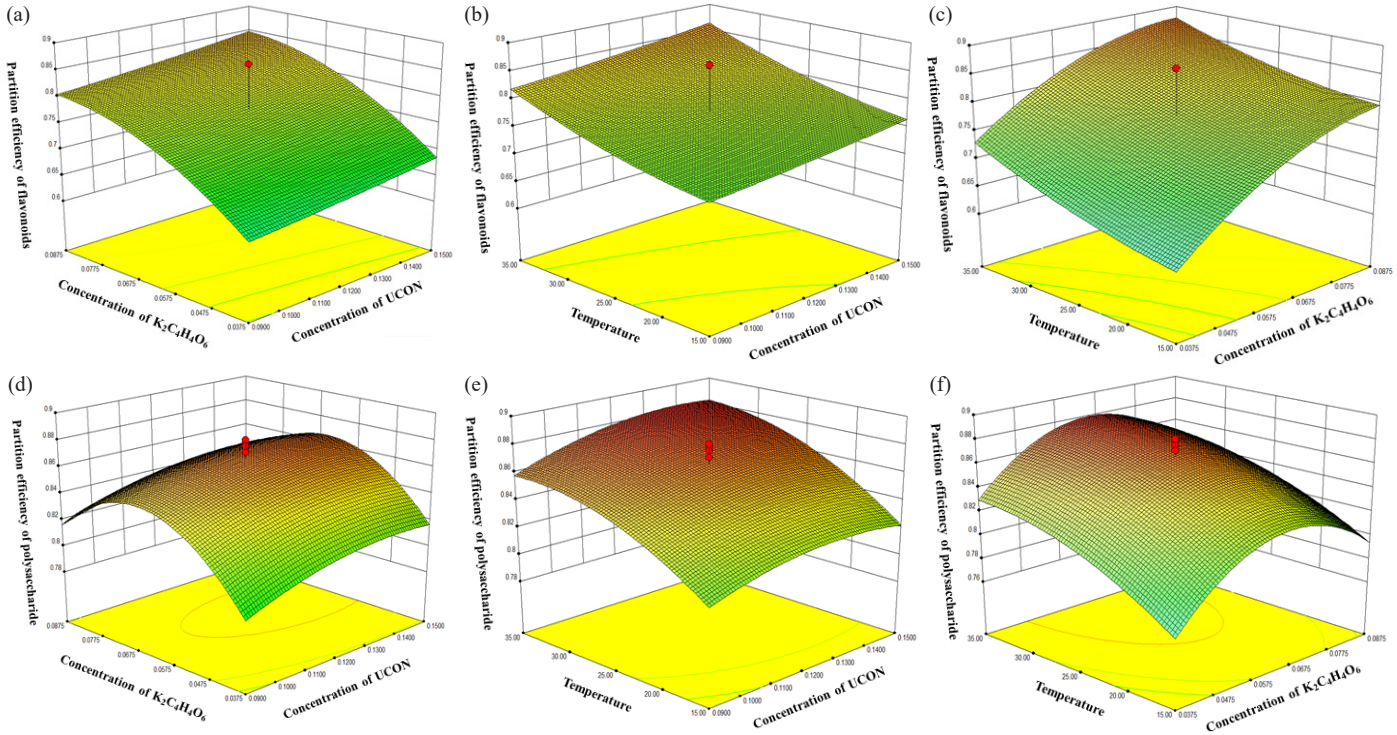

Figure 2 (a-f) The 3D response surface plot for the interactive effect of variables, while other variables are set at the fixed value.

3.5. The ANN model and prediction

3.5.1 Construction of ANN model

Three typical training algorithms, the Levenberg-Marquardt Algorithm, the Scaled Conjugate Gradient Algorithm, and the Bayesian Regularization Algorithm were used to form the ANN structure. The performances of the three algorithms were evaluated, and the results have been shown in Figure S7. The Levenberg-Marquardt Algorithm was used as the training algorithm for this ANN model. The input and output variables were normalized using three equations (Eqs. 9 to 11), and the regularized and original data were used to form the ANN model. Their performances have been listed in Table S6. The ANN model trained on the dataset normalized by Eq. (9) exhibited superior performance compared to those listed in Table S6. Therefore, Eq. (9) was used to normalize the input and output variables in this study. The hidden layer structure was the most important in the ANN model. The number of hidden neurons was varied from 3 to 45 in Step 3 to determine the optimal structure. The regression *R* values and epochs for the ANN model containing different hidden cells have been shown in Figure S8. Figure 3 shows the regression *R* values of the proposed ANN Model in the training, validation, test, and total datasets. The iterative time and MSE for each epoch have been shown in Figure S9.

3.5.2 Generalization ability

A completely unseen dataset was used to measure the generalization abilities of the two models proposed in this study. The unseen dataset was formed by collecting the partition efficiencies from the ATPS literature. The generalization abilities of the two models were evaluated using the mean relative percent difference (MRPD) values listed in Table S7. The ANN model was better than the RSM model in terms of the MRPD values. Moreover, the generalization ability of the ANN model was satisfactory for various factors, such as different types of ATPS, different objects, and different ranges of operational variables.

3.6. UCON recycling and cyclic test

The UCON-rich phase was transferred to a new test tube after ATPS formation. The UCON-rich phase was then diluted by adding water. The

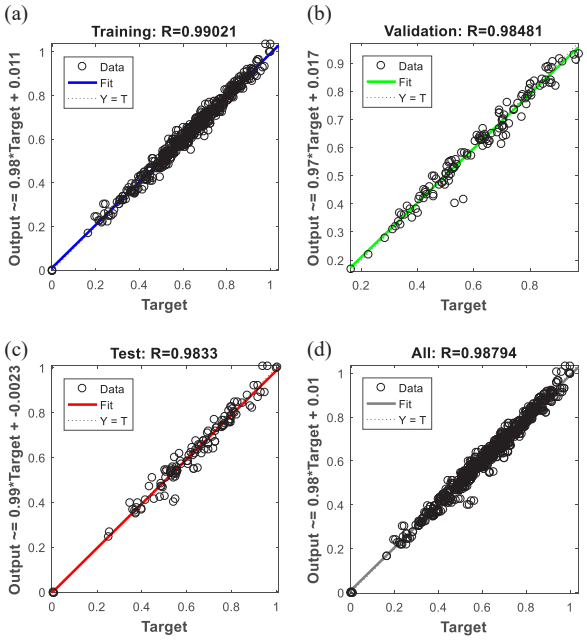

Figure 3. The regression R values of the proposed ANN Model in (a) the regression R values in training dataset, (b) the regression R values in validation dataset, (c) the regression R values in test dataset, (d) the regression R values in total dataset.

thermostat water bath which was maintained at 65°C of temperature was used to control the two phases forming. To determine the optimal recovery efficiency, the amount of added water was increased from 0.5 mL to 3.0 mL in 0.5 mL steps. On addition of, 2.0 mL water, the recovery efficiency reached its maximum value.

The recovered UCON was used as the main forming material in subsequent extraction experiments. The results of the three cycle tests have been presented in Table S8. It was found that the loss of UCON in each cycle test was about 0.4 mL from the table. This loss primarily resulted from the quantity needed for detection and unavoidable losses

during the transfer process. Additional EOPO was used to compensate for this shortfall in the subsequent ATPS extraction system. After the three extractions, the recovery of flavonoids increased gradually because flavonoid residues were present during each extraction. In each of these experiments, the recovery rate of flavonoids in the ATPS test was slightly higher than that in the UCON recovery experiment, and this was due to the wastage of flavonoids.

3.7. Validation of method

Two objects in seven groups of raw materials with different weights were extracted under optimum conditions. The partition and extraction performances have been listed in Table S9. The proposed method exhibited excellent partition and extraction performances in the range of raw material mass of 10-2000 g.

3.8. Purity and activity

The purities of the flavonoids and corn silk polysaccharides were determined under the optimum conditions. The purity of the flavonoids was between 98.19% and 99.27%, and that of the corn silk polysaccharide was between 98.46% and 99.73% (Table S10).

The antioxidant activities of flavonoids and corn silk polysaccharides were studied by evaluating their radical scavenging activities against DPPH, superoxide, and hydroxyl. The clearance rates have been shown in Figure 4. For the inhibitory on hydroxyl radical, the IC_{50} values of flavonoids and corn silk polysaccharides were 0.087 mg·mL^{-1} and 0.096 mg·mL^{-1}. It was reported that the scavenging effect of Vitamin C on hydroxyl radical was between 50% and 60% at 1.63 mg·mL^{-1}. For the inhibitory effects on DPPH radical, the IC_{50} values of flavonoids and corn silk polysaccharide were 0.069 mg·mL^{-1} and 0.025 mg·mL^{-1}, respectively. For the inhibitory on superoxide radical, the IC_{50} values of flavonoids and corn silk polysaccharide were 0.073 mg·mL^{-1} and 0.054 mg·mL^{-1}. Comparing the reported IC_{50} values of corn silk polysaccharide against DPPH (33.5 ug·mL^{-1}) and hydroxyl (102.7 ug·mL^{-1}) [16], and the IC_{50} values of polysaccharide against superoxide (0.06 mg·mL^{-1}) [57], the corn silk polysaccharide extracted by this method performed better.

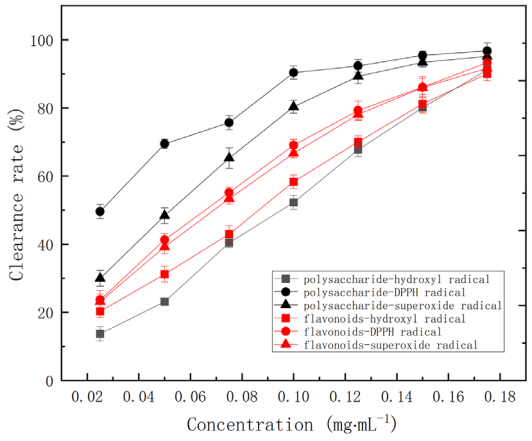

Figure 4. The antioxidant activities of the flavonoids and corn silk polysaccharides against DPPH, superoxide, and hydroxyl.

The DPPH activities of the flavonoids from astragalus membranaceus stems and leaves was given as IC_{50} values (0.149 mg·mL^{-1}) [53]. The IC_{50} value of flavonoids from kosteletzkya virginica root on superoxide radical was 0.078 mg·mL^{-1} [55]. Thus, the flavonoids from corn silk in this work have better antioxidant activity.

3.9. Comparison

3.9.1. Comparison of method

This method was compared with extraction methods described in previous literature, as shown in Table 1. This comparison may not be appropriate due to the differences in the samples from the listed literature. Nevertheless, it was concluded that this method was effective for the synchronous extraction and separation of flavonoids and corn silk polysaccharides from corn silk samples. The extraction efficiency proposed in this work was not only slightly higher than the extraction efficiency in other papers, but this method also has great practical application foreground because of its recycling.

3.9.2 Comparison of ANN model

The ANN model proposed in this study was compared with other reported ANN models, as listed in Table 2. The fitting and prediction performances of the ANN model on the dataset were evaluated using regression *R-value*. The generalization ability of the ANN model was measured using the MRPD value. The regression *R-value* of this ANN model was lower than those of the other three ANN models. We can obtain an ANN model with a better *R-value*; however, its generalization ability is weak. The proposed ANN model has a very good generalization ability according to the MRPD, which was obtained by computing data from the published literature. Furthermore, this ANN model has higher efficiency because of its two output responses.

Table 1. Comparison of different methods for extraction efficiency of three materials.

Method	Extraction efficiency (mg·g^{-1})		Recycling	References
	Flavonoids	Corn silk polysaccharide		
Ultrasound-assisted extraction	11.29	-	no	[58]
Ethanol extraction	-	13.10	no	[16]
Ethanol extraction	5.32	-	no	[59]
Ultrasound-assisted water extraction	-	60.60	no	[60]
Ultrasound-assisted ethanol extraction	-	71.00	no	[20]
Hot water extraction	-	29.47	no	[17]
Acid-assisted extraction	-	53.54	no	
Alkaline-assisted extraction	-	68.05	no	
Ultrasound-assisted extraction	-	20.40	no	
Ultrasound-assisted extraction	15.58	-		[61]
Proposed method	16.73	75.82	yes	This work

Table 2. Comparison of different ANN model.

ANN model	Number of hidden neurons			Number of data	R	MRPD		Ref
	Input layer	Hidden layer	Output layer			Own data	Data from published literatures	
Spent catalyst bioleaching	4	9-8	1	130	0.9880	-	-	[46]
High temperature deformation of alloy	3	10	1	208	0.9965	-	-	[50]
Hardness of alloy	6	6	1	16	0.9415	0.07	-	[49]
Properties of multiwall carbon nanotube fly ash	4	4	2	91	0.9996	0.14, 1.59	-	[48]
Tribological properties of polycarbonate composites	5	10-5	2	120	0.9375	-	-	[47]
Fatty acid methyl ester yield	4	10	1	162	0.9470	3.4	8.0～45.0	[45]
Partition efficiency of corn silk bioactive substance	3	18	3	282	0.9879	0.05	11.12～19.73	This model

4. Conclusions

The flavonoids and polysaccharides in corn silk were simultaneously extracted, separated, and analyzed using ultrasonic UCON Extraction combined with ATPS. The optimal experimental conditions were obtained through a multi-factor experiment designed by RSM. The average extraction efficiency of the flavonoid and polysaccharide reached 16.73 $mg \cdot g^{-1}$ and 75.82 $mg \cdot g^{-1}$. The UCON recycling experiment showed that UCON can be recycled and reused. This method has advantages for various applications owing to its good efficiency and recyclability. The partition efficiencies of the two object materials were predicted using ANN and RSM. The ANN prediction model performed well with both our data and those from other published studies, indicating that the ANN model has good generalization ability and can be used to predict the partition efficiency of other objects separated by different types of ATPS. Therefore, this method can simultaneously extract flavonoids and polysaccharides, as well as achieve separation, recovery, and reutilization of the extractant. Meanwhile, flavonoids and corn silk polysaccharides obtained by this method exhibit good antioxidant activities by evaluating their radical scavenging activities against DPPH, superoxide, and hydroxyl. The flavonoids and polysaccharides extracted from corn silk have great potential in the fields of the food, cosmetics and nutritional health supplement industries. This method offers a limited perspective simultaneous separation and extraction of other natural products. The ANN prediction model can enhance the research efficiency of separating natural products in ATPS. In further studies, the dynamic mechanism of the entire extraction process should be elucidated. Furthermore, the pharmacokinetic and pharmacodynamic properties of flavonoids and corn silk polysaccharides in vivo ought to be assessed. Further research is also needed on the changes in the contents of flavonoids and polysaccharides during the growth cycle.

CRediT authorship contribution statement

Jiawei Xu: Investigation, Formal Analysis, Writing – Original Draft; **Yang Lu:** Conceptualization, Methodology, Writing – review & editing, Funding acquisition.

Declaration of competing interest

The authors declare that they have no known competing financial interests or personal relationships that could have appeared to influence the work reported in this paper.

Declaration of Generative AI and AI-assisted technologies in the writing process

The authors confirm that there was no use of artificial intelligence (AI)-assisted technology for assisting in the writing or editing of the manuscript and no images were manipulated using AI.

Acknowledgment

This work was supported by the National Natural Science Foundation of China (No. 21606099), the Innovative and Entrepreneurial Talents Foundation of Jilin Province (No. 2023QN31) and the Natural Science Foundation of Jilin Province (No. YDZJ202301ZYTS157, 20240304097SF).

Supplementary data

Supplementary material to this article can be found online at https://dx.doi.org/10.25259/AJC_308_2024.

References

1. Wang, Y., Mao, J., Zhang, M., Liu, L., Zhu, Y., Gu, M., Zhang, J., Bu, H., Sun, Y., Sun, J., Ma, Y., Guo, L., Zheng, Y., Liu, Q., 2024. An umbrella insight into the phytochemistry features and biological activities of corn silk: A narrative review. *Molecules (Basel, Switzerland)*, **29**, 891. https://doi.org/10.3390/molecules29040891
2. Goyal, D., Jyoti, A., Kaur, M., Dhir, S., Rasane, P., Gunjal, M., Kaur, S., Ullah, R., Ercisli, S., Choudhary, R., Singh, J., 2024. Unveiling the therapeutic potential of corn silk against hypertension: A critical review. *Food Bioscience*, **62**, 105020. https://doi.org/10.1016/j.fbio.2024.105020
3. Li, Y., Hu, Z., Wang, X., Wu, M., Zhou, H., Zhang, Y., 2020. Characterization of a polysaccharide with antioxidant and anti-cervical cancer potentials from the corn silk cultivated in Jilin province. *International Journal of Biological Macromolecules*, **155**, 1105-1113. https://doi.org/10.1016/j.ijbiomac.2019.11.077
4. Tian, S., Sun, Y., Chen, Z., 2021. Extraction of flavonoids from corn silk and biological activities in vitro. *Journal of Food Quality*, **2021**, 1-9. https://doi.org/10.1155/2021/7390425
5. Zhang, D., Wang, Y., Liu, H., 2020. Corn silk extract inhibit the formation of N(epsilon)-carboxymethyllysine by scavenging glyoxal/methyl glyoxal in a casein glucose-fatty acid model system. *Food Chemistry*, **309**, 125708. https://doi.org/10.1016/j.foodchem.2019.125708
6. Huang, W., Ding, L., Zhang, N., Li, W., Koike, K., Qiu, F., 2021. Flavonoids from eucommia ulmoides and their in vitro hepatoprotective activities. *Natural Product Research*, **35**, 3584-3591. https://doi.org/10.1080/14786419.2020.1715402
7. Hussain, T., Tan, B., Rahu, N., Hussain Kalhoro, D., Dad, R., Yin, Y., 2017. Protective mechanism of eucommia ulmoids flavone (EUF) on enterocyte damage induced by LPS. *Free Radical Biology and Medicine*, **108**, S40. https://doi.org/10.1016/j.freeradbiomed.2017.04.152
8. Wang, X., Peng, M.-J., Wang, Z.-H., Yang, Q.-L., Peng, S., 2020. Ultrasound-microwave assisted extraction of flavonoid compounds from eucommia ulmoides leaves and an evaluation of their antioxidant and antibacterial activities. *Archives of Biological Sciences*, **72**, 211-221. https://doi.org/10.2298/abs191216015w
9. Ong, J.H., Koh, J.A., Cao, H., Tan, S.A., Abd Manan, F., Wong, F.C., Chai, T.T., 2021. Purification, identification and characterization of antioxidant peptides from corn silk tryptic hydrolysate: An integrated in vitro-in silico approach. *Antioxidants (Basel, Switzerland)*, **10**, 1822. https://doi.org/10.3390/antiox10111822
10. Zhang, L., Yang, Y., Wang, Z., 2021. Extraction optimization of polysaccharides from corn silk and their antioxidant activities in vitro and in vivo. *Frontiers in Pharmacology*, **12**, 738150. https://doi.org/10.3389/fphar.2021.738150
11. Wang, W., Yang, X., Tang, Y., Zhang, Y., Yue, S., 2024. The total tannins of geum japonicum thunb. var. Chinense extracted by green and natural deep eutectic solvent: Extraction optimization, component identification and hypoglycemic activity. *Industrial Crops and Products*, **222**, 119679. https://doi.org/10.1016/j.indcrop.2024.119679
12. Guo, L., Qiang, T., Yang, Y., He, Y., Dou, Y., Zhang, Z., Wu, T., Wang, H., 2024. Extraction and structural characterization of hydrolyzable tannins from coriaria nepalensis leaves. *Industrial Crops and Products*, **215**, 118646. https://doi.org/10.1016/j.indcrop.2024.118646
13. Wang, X., Li, H., Wang, S., Ruan, M., Li, Y., Zhu, L., Dong, Z., Long, Y., 2025. Genome-wide identification and functional roles relating to anthocyanin biosynthesis analysis in maize. *BMC Plant Biology*, **25**, 57. https://doi.org/10.1186/s12870-025-06053-4
14. Pashazadeh, H., Ali Redha, A., Johnson, J.B., Koca, I., 2025. Extraction optimization and microencapsulation of anthocyanins from okra flowers: Utilizing plant waste as a source of bioactive compounds. *Food Bioscience*, **63**, 105710. https://doi.org/10.1016/j.fbio.2024.105710
15. Kaur, P., Singh, J., Kaur, M., Rasane, P., Kaur, S., Kaur, J., Nanda, V., Mehta, C.M., Sowdhanya, D., 2023. Corn silk as an agricultural waste: A comprehensive review on its nutritional composition and bioactive potential. *Waste and Biomass Valorization*, **14**, 1413-1432. https://doi.org/10.1007/s12649-022-02016-0
16. Jia, Y., Xue, Z., Wang, Y., Lu, Y., Li, R., Li, N., Wang, Q., Zhang, M., Chen, H., 2021. Chemical structure and inhibition on alpha-glucosidase of polysaccharides from corn silk by fractional precipitation. *Carbohydrate Polymers*, **252**, 117185. https://doi.org/10.1016/j.carbpol.2020.117185
17. Jia, Y., Gao, X., Xue, Z., Wang, Y., Lu, Y., Zhang, M., Panichayupakaranant, P., Chen, H., 2020. Characterization, antioxidant activities, and inhibition on alpha-glucosidase activity of corn silk polysaccharides obtained by different extraction methods. *International Journal of Biological Macromolecules*, **163**, 1640-8. https://doi.org/10.1016/j.ijbiomac.2020.09.068
18. Smith, N.W., Evans, M.B., 1995. The efficient analysis of neutral and highly polar pharmaceutical compounds using reversed-phase and ion-exchange electrochromat, *Chromatographia*, **41**, 197-203. https://doi.org/10.1007/BF02267955
19. Biazus, J.P.M., Severo, J..B., Santana, J..C..C., Souza, R..R., Tambourgi, E..B., 2006. Study of amylases recovery from maize malt by ion-exchange expanded bed chromatography. *Process Biochemistry*, **41**, 1786-1791. https://doi.org/10.1016/j.procbio.2006.03.025
20. Chen, S., Chen, H., Tian, J., Wang, J., Wang, Y., Xing, L., 2014. Enzymolysis-ultrasonic assisted extraction, chemical characteristics and bioactivities of polysaccharides from corn silk. *Carbohydrate Polymers*, **101**, 332-341. https://doi.org/10.1016/j.carbpol.2013.09.046
21. Caminade, A.M., Hey-Hawkins, E., Manners, I., 2016. Smart inorganic polymers. *Chemical Society Reviews*, **45**, 5144-6. https://doi.org/10.1039/c6cs90086k
22. Yao, T., Feng, C., Yan, H., 2024. Current developments and applications of smart polymers based aqueous two-phase systems. *Microchemical Journal*, **204**, 111170. https://doi.org/10.1016/j.microc.2024.111170
23. Musarurwa, H., Tawanda Tavengwa, N., 2022. Recent progress in the application of pH-responsive polymers in separation science. *Microchemical Journal*, **179**, 107503. https://doi.org/10.1016/j.microc.2022.107503
24. Ma, Q., Zheng, X., 2022. Preparation and characterization of thermo-responsive composite for adsorption-based dehumidification and water harvesting. *Chemical Engineering Journal*, **429**, 132498. https://doi.org/10.1016/j.cej.2021.132498

25. Yao, T., Li, H., Yang, J., Shi, X., Yan, H., Peng, L., 2022. Determination and correlation of phase equilibria of chiral magnetic ionic liquid aqueous two-phase systems with different inorganic salts at 298.15 K. *Journal of Molecular Liquids*, **345**, 116983. https://doi.org/10.1016/j.molliq.2021.116983
26. Liu, H., Zhuang, S., Liang, C., He, J., Brennan, C.S., Brennan, M.A., Ma, L., Xiao, G., Chen, H., Wan, S., 2022. Effects of a polysaccharide extract from amomum villosum lour. on gastric mucosal injury and its potential underlying mechanism. *Carbohydrate Polymers*, **294**, 119822. https://doi.org/10.1016/j.carbpol.2022.119822
27. Yang, Y., Li, M., Sun, J., Qin, S., Diao, T., Bai, J., Li, Y., 2024. Microwave-assisted aqueous two-phase extraction of polysaccharides from hippophae rhamnoide l.: Modeling, characterization and hypoglycemic activity. *International Journal of Biological Macromolecules*, **254**, 127626. https://doi.org/10.1016/j.ijbiomac.2023.127626
28. Li, C., Belkin, D., Li, Y., Yan, P., Hu, M., Ge, N., Jiang, H., Montgomery, E., Lin, P., Wang, Z., Song, W., Strachan, J.P., Barnell, M., Wu, Q., Williams, R.S., Yang, J.J., Xia, Q., 2018. Efficient and self-adaptive in-situ learning in multilayer memristor neural networks. *Nature Communications*, **9**, 2385. https://doi.org/10.1038/s41467-018-04484-2
29. Grajciar, L., Heard, C.J., Bondarenko, A.A., Polynski, M.V., Meeprasert, J., Pidko, E.A., Nachtigall, P., 2018. Towards operando computational modeling in heterogeneous catalysis. *Chemical Society Reviews*, **47**, 8307-8348. https://doi.org/10.1039/c8cs00398j
30. Kite, S., Hattorib, T., Murakamib, Y., 1994. Estimation of catalytic performance by neural network - product distribution in oxidative dehydrogenation of ethylbenzene. *Applied Catalysis A: General*, **114**, 173-178. https://doi.org/10.1016/0926-860X(94)80169-X
31. Freire, M.G., Cláudio, A.F.M., Araújo, J.M.M., Coutinho, J.A.P., Marrucho, I.M., Lopes, J.N.C., Rebelo, L.P.N., 2012. Aqueous biphasic systems: A boost brought about by using ionic liquids. *Chemical Society Reviews*, **41**, 4966. https://doi.org/10.1039/c2cs35151j
32. Rito-Palomares, M., 2002. Process integration using aqueous two-phase partition for the recovery of intracellular proteins. *Chemical Engineering Journal*, **87**, 313-9. https://doi.org/10.1016/s1385-8947(01)00241-8
33. Desai, R.K., Streefland, M., Wijffels, R.H., H. M. Eppink, M., 2014. Extraction and stability of selected proteins in ionic liquid based aqueous two phase systems. *Green Chemistry*, **16**, 2670-9. https://doi.org/10.1039/c3gc42631a
34. Lu, Y., Lu, W., Wang, W., Guo, Q., Yang, Y., 2011. Thermodynamic studies of partitioning behavior of cytochrome c in ionic liquid-based aqueous two-phase system. *Talanta*, **85**, 1621-6. https://doi.org/10.1016/j.talanta.2011.06.058
35. Teixeira, A.G., Agarwal, R., Ko, K.R., Grant-Burt, J., Leung, B.M., Frampton, J.P., 2018. Emerging biotechnology applications of aqueous two-phase systems. *Advanced Healthcare Materials*, **7**, e1701036. https://doi.org/10.1002/adhm.201701036
36. Ao, G., Khripin, C.Y., Zheng, M., 2014. DNA-controlled partition of carbon nanotubes in polymer aqueous two-phase systems. *Journal of the American Chemical Society*, **136**, 10383-10392. https://doi.org/10.1021/ja504078b
37. Chao, Y., Shum, H.C., 2020. Emerging aqueous two-phase systems: From fundamentals of interfaces to biomedical applications. *Chemical Society reviews*, **49**, 114-142. https://doi.org/10.1039/c9cs00466a
38. da Silva, C.A., Coimbra, J.S., Rojas, E.E., Minim, L.A., da Silva, L.H., 2007. Partitioning of caseinomacropeptide in aqueous two-phase systems. *Journal of Chromatography. B, Analytical Technologies in the Biomedical and Life Sciences*, **858**, 205-210. https://doi.org/10.1016/j.jchromb.2007.08.033
39. Sharma, V., Joo, J.U., Mottafegh, A., Kim, D.P., 2024. Continuous and autonomous-flow separation of laccase enzyme utilizing functionalized aqueous two-phase system with computer vision control. *Bioresource Technology*, **403**, 130888. https://doi.org/10.1016/j.biortech.2024.130888
40. Tue, N.H., Phuc, N.H., Hoa, P.T.B., Tien, N.Q.D., Loc, N.H., 2024. Partitioning recombinant chitinase from nicotiana benthamiana by an aqueous two-phase system based on polyethylene glycol and phosphate salts. *International Journal of Biological Macromolecules*, **269**, 131924. https://doi.org/10.1016/j.ijbiomac.2024.131924
41. Yu, W., Li, K., Liu, Z., Zhang, H., Jin, X., 2018. Novelty aqueous two-phase extraction system based on ionic liquid for determination of sulfonamides in blood coupled with high-performance liquid chromatography. *Microchemical Journal*, **136**, 263-9. https://doi.org/10.1016/j.microc.2017.03.053
42. Li, L.-H., Li, F.-F., 2012. Chiral separation of α-cyclohexyl-mandelic-acid by aqueous two phase system combined with Cu2-β-cyclodextrin complex. *Chemical Engineering Journal*, **211-212**, 240-5. https://doi.org/10.1016/j.cej.2012.09.058
43. Fan, L., Li, W., Dai, Z., Zhou, M., Qiu, Y., 2024. Efficient separation of re (VII) and mo (VI) by extraction using e-1006–Ammonium sulfate aqueous two-phase system. *Separations*, **11**, 142. https://doi.org/10.3390/separations11050142
44. Shibukawa, M., Hirasawa, T., Saito, S., 2024. Structure of polyethylene glycol/water mixtures as a separation medium of aqueous two-phase extraction systems studied by equilibrium analysis of thiocyanato complexation of cobalt(II). *Polymer*, **293**, 126658. https://doi.org/10.1016/j.polymer.2023.126658
45. Rajković, K.M., Avramović, J.M., Milić, P.S., Stamenković, O.S., Veljković, V.B., 2013. Optimization of ultrasound-assisted base-catalyzed methanolysis of sunflower oil using response surface and artifical neural network methodologies. *Chemical Engineering Journal*, **215-216**, 82-9. https://doi.org/10.1016/j.cej.2012.10.069
46. Vyas, S., Das, S., Ting, Y.-P., 2020. Predictive modeling and response analysis of spent catalyst bioleaching using artificial neural network. *Bioresource Technology Reports*, **9**, 100389. https://doi.org/10.1016/j.biteb.2020.100389
47. Zakaulla, M., Parveen, F., Amreen, , Harish, , Ahmad, N., 2020. Artificial neural network based prediction on tribological properties of polycarbonate composites reinforced with graphene and boron carbide particle. *Materials Today: Proceedings*, **26**, 296-304. https://doi.org/10.1016/j.matpr.2019.11.276
48. Devadiga, U., Poojary, R.K.R., Fernandes, P., 2019. Artificial neural network technique to predict the properties of multiwall carbon nanotube-fly ash reinforced aluminium composite. *Journal of Materials Research and Technology*, **8**, 3970-7. https://doi.org/10.1016/j.jmrt.2019.07.005
49. Dewangan, S.K., Samal, S., Kumar, V., 2020. Microstructure exploration and an artificial neural network approach for hardness prediction in alCrFeMnNiWx high-entropy alloys. *Journal of Alloys and Compounds*, **823**, 153766. https://doi.org/10.1016/j.jallcom.2020.153766
50. Adarsh, S..H., Sampath, V., 2020. Prediction of high temperature deformation characteristics of an fe-based shape memory alloy using constitutive and artificial neural network modelling. *Materials Today Communications*, **22**, 100841. https://doi.org/10.1016/j.mtcomm.2019.100841
51. Sui, M., Feng, S., Liu, G., Chen, B., Li, Z., Shao, P., 2023. Deep eutectic solvent on extraction of flavonoid glycosides from dendrobium officinale and rapid identification with UPLC-triple-TOF/MS. *Food Chemistry*, **401**, 134054. https://doi.org/10.1016/j.foodchem.2022.134054
52. Zhu, L., Lu, Y., Sun, Z., Han, J., Tan, Z., 2020. The application of an aqueous two-phase system combined with ultrasonic cell disruption extraction and HPLC in the simultaneous separation and analysis of solanine and solanum nigrum polysaccharide from solanum nigrum unripe fruit. *Food Chemistry*, **304**, 125383. https://doi.org/10.1016/j.foodchem.2019.125383
53. Cui, L., Ma, Z., Wang, D., Niu, Y., 2022. Ultrasound-assisted extraction, optimization, isolation, and antioxidant activity analysis of flavonoids from astragalus membranaceus stems and leaves. *Ultrasonics Sonochemistry*, **90**, 106190. https://doi.org/10.1016/j.ultsonch.2022.106190
54. Zhang, Y., Cao, C., Yang, Z., Jia, G., Liu, X., Li, X., Cui, Z., Li, A., 2023. Simultaneous determination of 20 phenolic compounds in propolis by HPLC-UV and HPLC-MS/MS. *Journal of Food Composition and Analysis*, **115**, 104877. https://doi.org/10.1016/j.jfca.2022.104877
55. Zai, Y., Liu, S., 2023. Extraction, antioxidant activity and identification of flavonoids from root tubers of kosteletzkya virginica. *Phyton*, **92**, 225-236. https://doi.org/10.32604/phyton.2022.022576
56. Rico-Castro, X., González-Amado, M., Soto, A., Rodríguez, O., 2017. Aqueous two-phase systems with thermo-sensitive EOPO co-polymer (UCON) and sulfate salts: Effect of temperature and cation. *The Journal of Chemical Thermodynamics*, **108**, 136-142. https://doi.org/10.1016/j.jct.2017.01.009
57. Zhang, Q., Yu, P., Li, Z., Zhang, H., Xu, Z., Li, P., 2003. Antioxidant activities of sulfated polysaccharide fractions from Porphyra haitanesis, *Journal of Applied Phycology*, **15**, 305-310.
58. Hu, X., Yang, T., Qi, X., Guo, X., Hu, J., 2022. Effects of different drying methods on phenolic composition and antioxidant activity in corn silk (Stigma maydis). *Journal of Food Processing and Preservation*, **46**, 17101-17107. https://doi.org/10.1111/jfpp.17101
59. Wu, J., Ye, M., Wang, Z., 2017. Extraction, purification and anti-hyperlipidemic activities of total flavonoids from corn silk. *Pakistan Journal of Zoology*, **49**. https://doi.org/10.17582/journal.pjz/2017.49.6.2173.2179
60. Prakash Maran, J., Manikandan, S., Thirugnanasambandham, K., Vigna Nivetha, C., Dinesh, R., 2013. Box-behnken design based statistical modeling for ultrasound-assisted extraction of corn silk polysaccharide. *Carbohydrate Polymers*, **92**, 604-611. https://doi.org/10.1016/j.carbpol.2012.09.020
61. Zheng, L.-L., Wen, G., Yuan, M.-Y., Gao, F., 2016. Ultrasound-assisted extraction of total flavonoids from corn silk and their antioxidant activity. *Journal of Chemistry*, **2016**, 1-5. https://doi.org/10.1155/2016/8768130